FFI RAPPORT

POLARIZATION DEPENDENCE IN CHESS FIBER OPTIC STRAIN MONITORING SYSTEM BASED ON FIBER BRAGG GRATINGS

VINES Lasse

FFI/RAPPORT-2002/03348

FFIE/793/116

Approved
Kjeller 21. August 2002

Stian Løvold
Director of Research

POLARIZATION DEPENDENCE IN CHESS FIBER OPTIC STRAIN MONITORING SYSTEM BASED ON FIBER BRAGG GRATINGS

VINES Lasse

FFI/RAPPORT-2002/03348

FORSVARETS FORSKNINGSINSTITUTT
Norwegian Defence Research Establishment
P O Box 25, NO-2027 Kjeller, Norway

FORSVARETS FORSKNINGSINSTITUTT (FFI)
Norwegian Defence Research Establishment

P O BOX 25
N0-2027 KJELLER, NORWAY

UNCLASSIFIED

SECURITY CLASSIFICATION OF THIS PAGE (when data entered)

REPORT DOCUMENTATION PAGE

1) PUBL/REPORT NUMBER	2) SECURITY CLASSIFICATION	3) NUMBER OF PAGES
FFI/RAPPORT-2002/03348	UNCLASSIFIED	25
1a) PROJECT REFERENCE	**2a) DECLASSIFICATION/DOWNGRADING SCHEDULE**	
FFIE/793/116	-	

4) TITLE

POLARIZATION DEPENDENCE IN CHESS FIBER OPTIC STRAIN MONITORING SYSTEM BASED ON FIBER BRAGG GRATINGS

5) NAMES OF AUTHOR(S) IN FULL (surname first)

VINES Lasse

6) DISTRIBUTION STATEMENT

Approved for public release. Distribution unlimited. (Offentlig tilgjengelig)

7) INDEXING TERMS

IN ENGLISH:	IN NORWEGIAN:
a) Bragg gratings	a) Bragg gittere
b) Polarisation	b) Polarisasjon
c) Superluminescent diodes	c) Superluminesente dioder
d)	d)
e)	e)

THESAURUS REFERENCE: **INSPEC Thesaurus 1999**

8) ABSTRACT

This report describes the polarization dependence in the hull monitoring system CHESS, developed in FFI project 79301 CHESS II. The report describes the polarization behaviour of some main components in the system, and describes a depolarizer for reducing unwanted polarization effects in the system. The latter part of this report contains experimental investigations for identifying unwanted polarization effects and demonstrates how these effects can be reduced.

9) DATE	AUTHORIZED BY This page only	POSITION
21. August 2002	Stian Løvold	Director of Research

ISBN-82-464-0645-0

UNCLASSIFIED

SECURITY CLASSIFICATION OF THIS PAGE (when data entered)

CONTENTS

PAGE

1	INTRODUCTION	7
2	THEORETICAL BACKGROUND	7
2.1	Optical network in hull monitoring system	7
2.2	Superluminecent light emitting diodes	7
2.3	Polarization considerations in Fiber Bragg Gratings	8
2.4	Depolarizer	10
3	POLARIZATION TESTS IN STRAIN MEASURING SYSTEM	13
3.1	Degree of Polarization	13
3.2	Experimental Setup	15
3.3	Impact of sources	16
3.4	Impact of gratings	18
3.5	Depolarizer	20
4	CONCLUSIONS	23
	References	23
	Distribution list	25

This page is intentionally left blank.

POLARIZATION DEPENDENCE IN CHESS FIBER OPTIC STRAIN MONITORING SYSTEM BASED ON FIBER BRAGG GRATINGS

1 INTRODUCTION

This report describes the polarization characteristics of the CHESS Hull Monitoring System [1]. The system uses Fiber-optic Bragg Gratings (FBG) as sensors, measuring strain in the structure under investigation, in this case the hull of a ship.

The basic idea is measurement of wavelength, or change of wavelength of the reflected light from the FBG. Since one measures wavelength in a non-interferometric system, polarization effects was not considered in the preliminary studies. But, while testing the system, effects which could remind of polarization effects were observed, and further studies of polarization effects in the system was needed.

A virtual strain-signal was observed when the state of polarization (SOP) in the fiber network was altered. This report identifies the cause of this behavior, quantifies the polarization dependence in the CHESS system, and propose a solution that reduces this effect.

Chapter 2 gives a brief overview of the optical part of the Hull Monitoring system, and describes the most crucial components for the polarization behavior of the system. A depolarizer is also described, since it is a possible solution to the problems observed. Chapter 3 reports the tests performed, while Chapter 4 discusses the result of the tests.

2 THEORETICAL BACKGROUND

2.1 Optical network in hull monitoring system

The interrogation system of the Hull Monitoring System is given in [2]. The optical part of the hull monitoring system is shown in Figure 2.1

Light from a broad banded source (FWHM $\sim 30nm$) enters an isolator before the tunable filter, to avoid degradation of the source due to backreflection. The Fabry-Perot tunable filter has a passband of 0.2 nm, and scans contionusly over the entire wavelength range. The output of the filter is connected to an optical network, consisting of one 1x8 coupler and 8 2x2 couplers. The first coupler splits the light into 8 channels, and the reflected light from each FBG is detected after the 2x2 couplers.

2.2 Superluminecent light emitting diodes

The hull monitoring system described above, relies on a broad band source . Superluminescent diodes (SLD) and Erbium Doped Fiber Amplifiers (EDFA) are suitable

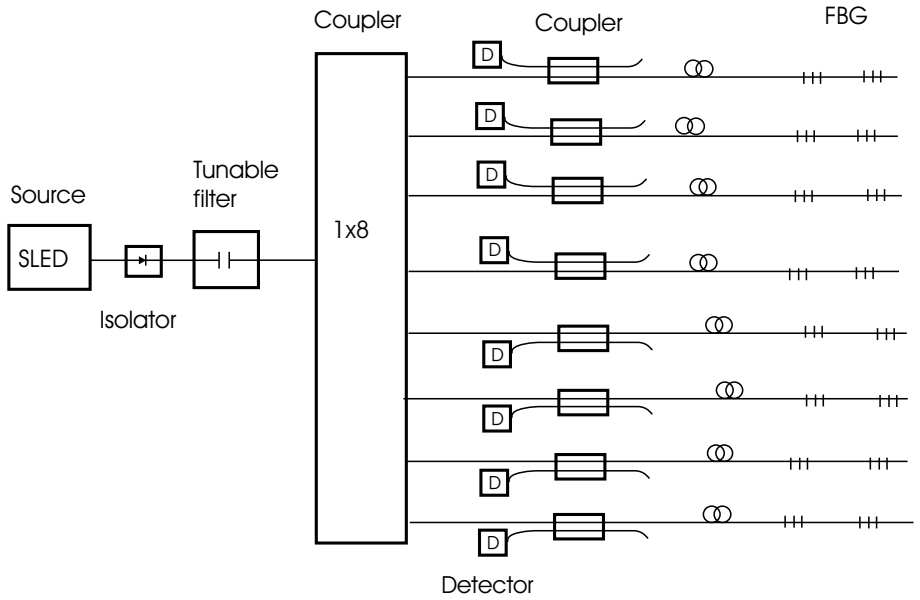

Figure 2.1: Schematic overview of the optical network in the hull monitoring system(CHESS)

sources, where SLDs have been preferred of cost reasons.

Conventional superluminescent diodes consist of double-heterostructure (DH) material (e.g. GaAs/AlGaAs) [3], but diodes based on quantum wells (QW) or quantum dots (QD) are available as well. The optical feedback in the diode is supressed by decreasing the reflectivity of the mirror facets with an antireflection coating, using absorbing material in regions of the diode, or by introducing angled stripe goemetry, i.e. cleave the edge by an angle β. An ordinary design uses antireflection coating at the emission output edge, and an absorbing region at the other diode end.

The device will consequently amplify spontaneous emission only along a single pass. The result is a broad spectrum ($\sim 30nm$) with relatively high output power (compared to LEDs, $> 1mW$). The spectrum stability is poor, resulting in a temperature drift $\sim 400ppm/K$ of the peak wavelength and a drift due to driving current $\sim 40ppm/mA$. A temperature controller is therefore usually implemented in the source unit.

SLDs are partially polarized sources with up to 80% of the power in the polarization parallel to the junction. The reason for the high degree of polarization is mainly due to different mode confinement factors for the TE and TM modes.

2.3 Polarization considerations in Fiber Bragg Gratings

The strain sensor development and technology of the CHESS Hull Monitoring System are described in [4] [5].

It will be shown in Chapter 3 that when a polarized or partially polarized source is used in the CHESS system, the system can be polarization dependent when the FBG is birefringent. If the strain transfer from the primary coating to the fiber is not uniform, birefringence will

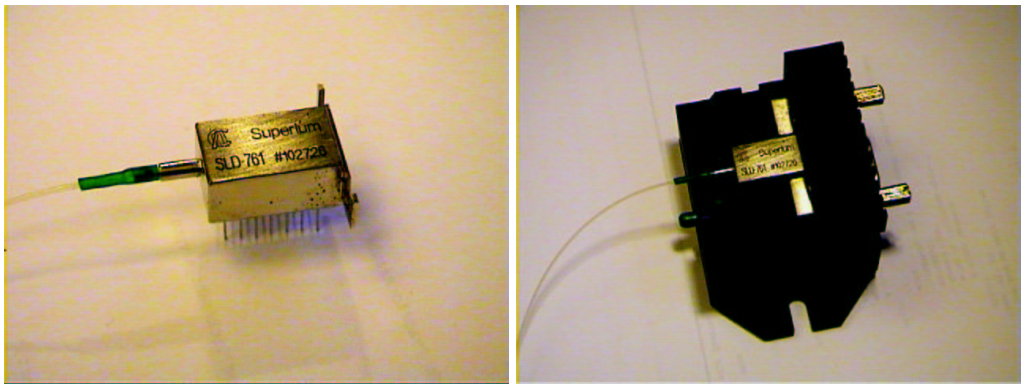

Figure 2.2: SLD with fiber pigtail produced by Superlum Ltd. The right picture shows the SLD mounted on a temperature controller

be introduced to the FBG. Different input SOP to a birefringent FBG will experience different index of refraction (IOR), thus the Bragg wavelength for light polarized along the two principal axes will be different. When the input SOP changes with time, the reflected wavelength will change with time, and this is interpreted as a strain signal. The non-uniform strain transfer from the primary coating to the fiber can originate from curvature of the fiber, stress introduced by the strain transfer material (e.q. adhesive and polyimide films), or from the primary coating itself (strain introduced under recoating). The birefringence can also be inherent in the fiber itself (induced under manufacturing), e.g. if the fiber is not perfectly circular.

The FBG used as strain sensors are fixed to the polyimide films in a straight line, so little birefringence should be introduced by curvature of the fiber. But, it is likely that the strain-transfer film will introduce birefringence, e.g. the amount of adhesive on each side of the FBG is different, introducing stress in the primary coating in the curing process. On the other hand, in the strain isolated packages for temperature compensation, only a curvature of the FBG is introduced (no coating besides the primary coating is used).

To aquire some knowledge about the magnitude of the polarization effect described above, consider the FBG in the strain isolated package. The loop introduce curvature and consequently birefringence in a fiber. The change in index of refraction depends on the radius of the loop and the radius of the fiber (with coating). The relation can be shown to be [6]

$$\Delta n = a\frac{r^2}{R^2} \tag{2.1}$$

Here Δn is the change in index of refraction between the largest and smallest IOR (the two principal axes of polarization), a is a constant, r is the radius of the fiber and R is the radius of the loop. Birefringence in the direction of the fiber (normal to R) is neglible.

In the hull monitoring system, the FBG used as temperature sensors are put in a circular groove with diameter 3 cm in a PVC plate. Each end of the fiber in the loop are glued to the PVC, and the fiber is covered with a lid. The FBG therefore has the shape of an arc, and this

bending result in birefringence in the fiber in the transversal direction of the fiber. With $r = 125\mu m$, $a \cong 0.133$ and $R = 15mm$, a typical number for the change in IOR is found:

$$\Delta n = 9.24 \cdot 10^{-6} \tag{2.2}$$

The Bragg condition is given by

$$\begin{aligned} &\lambda = 2n_{eff} \cdot \Lambda \\ &\Rightarrow \ \Delta\lambda = 2\Delta n \cdot \Lambda \end{aligned} \tag{2.3}$$

where λ is the Bragg wavelength (the wavelength of the reflected light), n_{eff} is the effective IOR and Λ is the modulation period of the grating. By using $n_{eff} = 1.5$, and $\lambda = 1550nm$, the modulation period becomes $\Lambda = 5.31 \cdot 10^{-7}$m, and the change in IOR due to the circular shape of the FBG becomes

$$\Delta\lambda = 9.24 \cdot 10^{-6} \cdot 2 \cdot 5.31 \cdot 10^{-7} m = 9.81pm \tag{2.4}$$

This value corresponds to $8.2\mu\epsilon$.

In conclusion, a circular shape of the grating result in a change in the Bragg condition in the radial direction. The wavelength of the reflected light will therefore depend on the polarization of the light, since different SOPs will see different IOR. In the worst case, a change of $9.81pm$ in wavelength will be seen (totally polarized light). It is likely that a similar effect would appear in the FBG prepacked in polyimide films.

2.4 Depolarizer

A possible solution to the polarization problem is using depolarized light. The reflection spectrum from a birefringent FBG would then be the sum of the reflection spectrum from each of the principal axes of polarization. The reflection spectrum using depolarized light will consequently be slightly broader than for a FBG using polarized light (unless the polarization is linearly polarized and 45^o compared to the principal axis of polarization, or the light is circularly polarized), but the spectrum will not change with external effects working on the fiber outside the grating.

Polarized light can be depolarized using different depolarizing techniques. The Lyot type depolarizer [7] requires a broad band source, and gives each spectral component in the broad band light a random SOP, so that the sum of all the spectral components appears depolarized. Since the reflection spectrum of the FBG is relatively narrow band, $\Delta\lambda_{FWHM} = 0.1nm$, compared to the requirements of the Lyot type depolarizer ($\Delta\lambda > 15nm$), this component is not suited for the application at hand.

A passive fiber depolarizer for sources with smaller bandwidths are suggested in [8],[9]. The basis of such a depolarizer is a 2x2 coupler, where one output fiber is coupled to one of its own input fibers (see Figure 2.3).

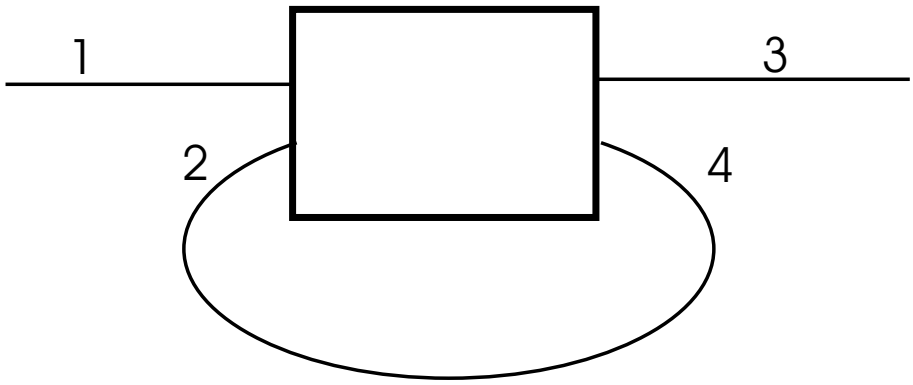

Figure 2.3: Schematics of a depolarizer

A section of a single mode fiber can be modeled by a combination of a discrete linear $R_l(\delta_l, \theta)$ and a circular $R_c(\delta_c)$ retarder.

$$R_l(\delta_l, \theta) = \begin{bmatrix} e^{i\delta_l/2}\cos^2(\theta) + e^{-i\delta_l/2}\sin^2(\theta) & 2i\sin(\theta)\cos(\theta)\sin(\delta_l/2) \\ 2i\sin(\theta)\cos(\theta)\sin(\delta_l/2) & e^{-i\delta_l/2}\cos^2(\theta) + e^{i\delta_l/2}\sin^2(theta) \end{bmatrix} \tag{2.5}$$

$$R_c(\delta_c) = \begin{bmatrix} \cos(\frac{\delta_c}{2}) & \sin(\frac{\delta_c}{2}) \\ -\sin(\frac{\delta_c}{2}) & \cos(\frac{\delta_c}{2}) \end{bmatrix} \tag{2.6}$$

Here δ_l is the linear retardation, θ is the azimuth of the fast axis of the linear retarder, and δ_c is the circular retardation.

We assume that no interference effects occur, that is

$$L_d >> L_{coh} \tag{2.7}$$

where L_d is the length of the fiber connecting output arm 4 with input arm 2, and L_{coh} is the coherence length of the incoming light.

If we also assume no loss in the system, we can write the electric field E_{out} at the output as

$$E_{out} = E_0 + E_1 + E_2 + ... + E_n \tag{2.8}$$

where E_0 is the part of the incident light coupled directly between port 1 and 3, E_1 is the part of the light propagating only one time through the feedback loop, E_2 propagates two times in the feedback loop, and so on.

By defining the transfer matrix for direct coupling, K_d, coupling between port 1 and 3 or 2 and 4, and cross coupling K_c (coupling between port 1 and 4 or 2 and 3)

$$K_d = \begin{bmatrix} \sqrt{1-k} & 0 \\ 0 & \sqrt{1-k} \end{bmatrix} \tag{2.9}$$

$$K_c = \begin{bmatrix} \sqrt{k} & 0 \\ 0 & \sqrt{k} \end{bmatrix} \tag{2.10}$$

where $J = R_l(\delta_l, \theta)R_c(\delta_c)$ is the birefringence matrix, k is a coupling parameter (value between 0 and 1). The electric field in Equation 2.8 can now be written as

$$\begin{aligned} E_0 &= K_d E_i \\ E_1 &= K_c J K_c E_i \\ E_2 &= K_c J K_d J K_c E_i \\ &\vdots \\ E_n &= K_c (J K_d)^{n-1} J K_c E_i \end{aligned} \tag{2.11}$$

The intensity at the output becomes

$$I_{out} =< |E_{out}|^2 >= |E_0|^2 + |E_1|^2 + |E_2|^2 + .. + |E_n|^2 = I_{in} \tag{2.12}$$

One can observe that the output wave is a superposition of different polarization states given that $J \neq 0$. For only one 2x2 coupler, the strongest wave , E_0 will be half the input power, thus the system will depolarize the incident light by no more than a factor 2. Higher degree of depolarization can be obtained by using a cascade of 2x2 couplers, as shown in Figure 2.4. As more depolarization units are added, a higher degree of depolarization is accomplished, assuming each depolarizer (2x2 coupler with feedback loop) to have a different J. Each feedback loop must also have different length ($L_{d,i} - L_{d,j} >> L_{coh}$ for $i \neq j$) to avoid interference effects.

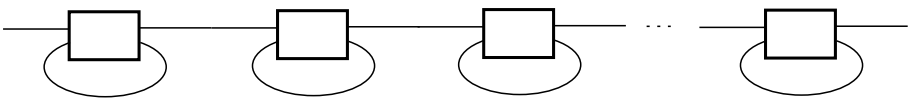

Figure 2.4: Cascade of 2x2 depolarizers

If the input polarization is known, a complete depolarization is possible by two 2x2 depolarizers with polarization controllers in the feedback loops (controlling the change in SOP in the feedback loop, J) [10]. The disadvantage of this design is the need for a stable input polarization. This is difficult in the hull monitoring system, where the system is expected to operate over a long period of time with temperature changes and vibrations.

The couplers do not have to be 2x2 couplers, other couplers can be used as well, such as 3x3 or 8x8 couplers. A 3x3 coupler will give better depolarization than a 2x2 coupler, due

to reduced intensity in the E_0 wave and increased number of possible couping combinations. The drawback using multiport couplers are the increased cost and increased loss in the coupler.

3 POLARIZATION TESTS IN STRAIN MEASURING SYSTEM

3.1 Degree of Polarization

The Degree Of Polarization (DOP) was measured using a Polarization Analyzer from Profile Optische Systeme (PAT 9000b). The analyzer uses a Jones-Matrix technique, and relies on a Polarimeter. Since the polarimeter assumes a narrow band source, a broader source gives some errors in the measurements, but the inaccuracies are assumed to be neglible in these tests.

The experimental setup is shown in Figure 3.1

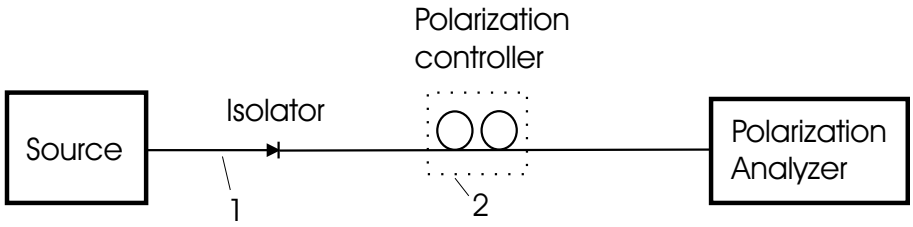

Figure 3.1: Setup for DOP measurement

A systematic change in the state of polarization (SOP) is introduced to fiber 2 (in Figure 3.1) using a Polarization controller, see Figure 3.2.

A change in SOP in fiber 1 (in Figure 3.1), i.e. before the isolator, gives a much larger change in DOP, see Figure 3.3

The measured values varied significantly between measurements, but typical values are given in Table 3.1 below

Source	typical value of DOP	variation
Superlum	70%	15% - 80 %
Opto Speed	60%	15% - 80%
Erbium	$< 1\%$	

Table 3.1: Output DOP from different broad banded sources

From Figure 3.3 one can observe that the source is very sensitive to effects changing the SOP in the fiber in front of the isolator. One possible reason for this behavior is the influence of the backscattered and reflected light on the source. Changing the SOP in the output fiber also changes the SOP of the backreflected and backscattered light. Some of this light enters the source and changes the polarization characteristics of the source.

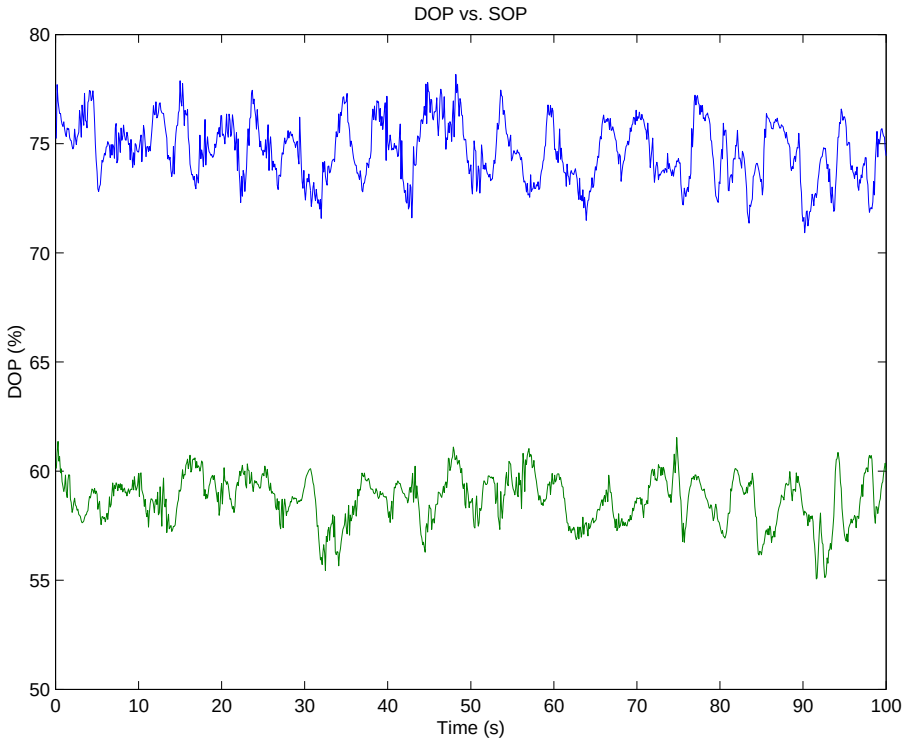

Figure 3.2: DOP vs. SOP (SOP are changed as a function of time) for Opto Speed and Superlum source

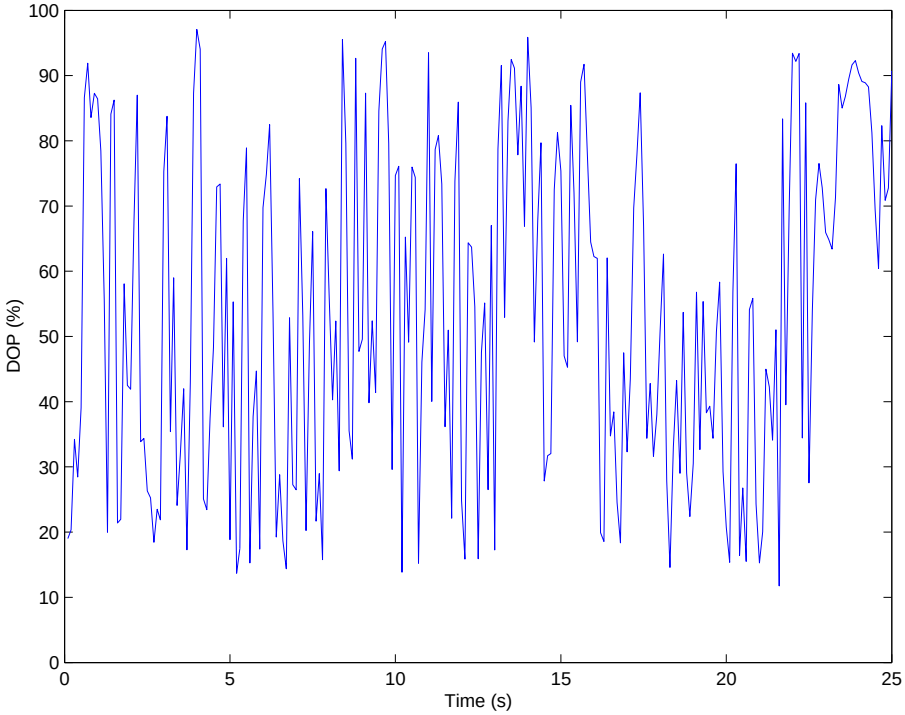

Figure 3.3: DOP vs. SOP (SOP is systematically changed with time) for Opto Speed source when changes in SOP are introduced in front of the isolator

Changes in the SOP after the isolator are also observable, but at a much smaller scale, since only a small portion of the backreflected light reaches the source (extinction ratio of the isolator =40dB).

The discussion above indicates that it is possible to control the DOP by controlling the SOP of the backreflected light. One problem here is the polarization fluctuation. The SOP changes slowly over time, and a feedback loop is necessary to keep a steady DOP. This is illustrated in Figure 3.4, and 3.5 where a polarization controller was used to tune the output DOP to around 18%, and then left alone.

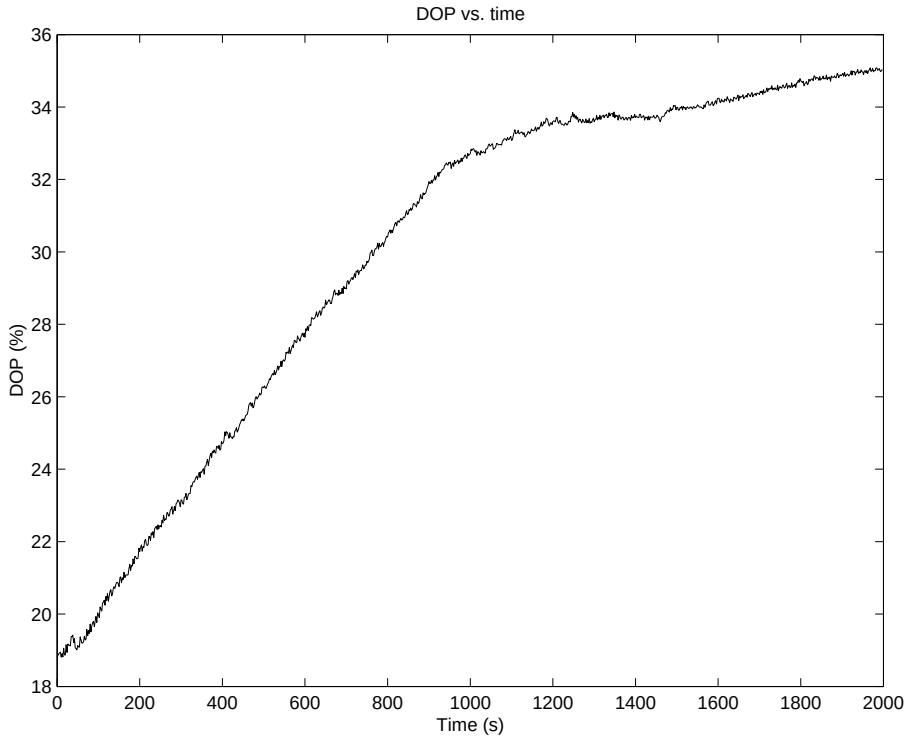

Figure 3.4: DOP vs. time showing the influence of polarization fading on the degree of polarization

In the first test, the DOP changed significantly over half an hour, while in the second test, only small variations were observed during 17 hours. These tests show the unpredictability of the polarization. The first test was made during daytime when people were working nearby, while the second test (Figure 3.5) was made over night when no one was in the room were the test was perfomed. In the hull monitoring application, one can not expect the DOP to be as stable as the second test due to temperature variations and motion of the vessel.

3.2 Experimental Setup

The tests described in the next sections were performed in the following way. The hull monitoring system was set up as described in Chapter 2.1. A polarization controller (pc) was introduced after the isolator, and set to scan continously over all possible states of polarization (SOP). The scan rate of the polarization controller was 10s, i.e. the pc uses 10

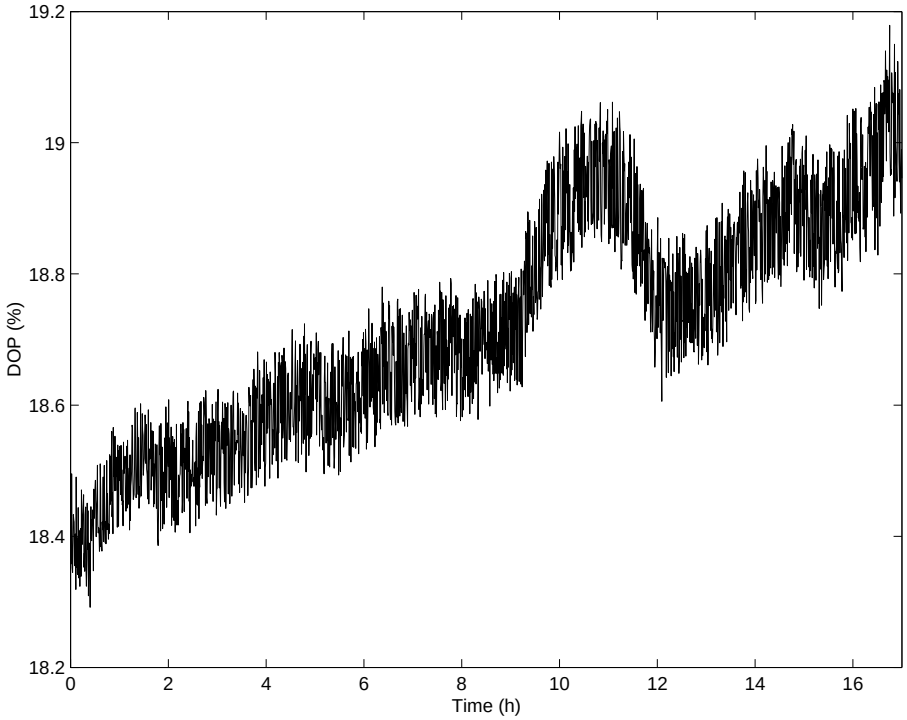

Figure 3.5: DOP vs. time showing the influence of polarization fading on the degree of polarization

seconds to change one input SOP to all possible output SOP's. For each test, a 30s sample was recorded.

The idea is that the polarization controller will simulate external effects working on the optical system changing the SOP. If no additional strain is applied to the system, except from the strain introduced during production, measured strain from the readout unit can be traced back to the change in polarization.

3.3 Impact of sources

Three different sources were tested, two superluminescent light emitting diodes (SLD) from different manufacturers (Superlum Ltd. and Opto Speed), and one Erbium Doped Fiber Amplifier (EDFA) source. The EDFA source was tested for verification purposes, since it emits depolarized light.

Measured strain from one sensor (strain sensor prepacked in polymide film) using different sources are shown in Table 3.2 and Figure 3.6

Changing the polarization does not affect the measured strain while the erbium source was used. The reason is that since each frequency component has an arbitrary polarization, the polarization will still be arbitrary after the polarization controller. The SLD from superlum gave larger measured strain error than the SLD from Opto Speed. The reason can be a difference in DOP between the two sources, since it has been shown that the DOP from both sources can vary significantly between measurements.

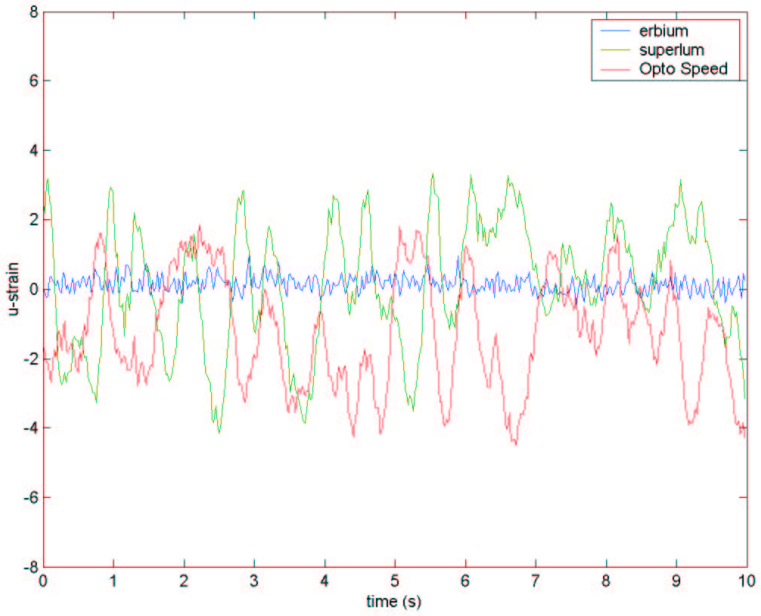

Figure 3.6: changes in measured strain as a function of SOP

Source	$\epsilon_{max} - \epsilon_{min} (\mu\epsilon)$
Superlum	7.7
Opto Speed	6.8
EDFA	1.8

Table 3.2: Typical values for changes in measured change as a function of input SOP to a FBG prepacked in polymide film

3.4 Impact of gratings

In the following tests, only the Opto Speed source was used. First, we examine the consequence of curvature to a FBG. Figure 3.7 below shows a 10 sec. sample from one of the tests. Temperature sensors 1 to 4 are all put in a circular groove in an aluminium plate. The temperature of the aluminium plate is controlled by a Peltier element. The diameter of the groove is 3 cm. Temperature sensors should consequently show no response to changes in the (external) temperature. The unstrained FBG are flexible attached (not glued) to a glass plate. This sensor should consequently not experience any birefringence except from the birefringence induced during manufacturing, but will be exposed to temperature changes, although these temperature changes are expected to be negligible over the time of test.

The results from a 30 s sample are shown Table 3.3, with a 10s section of this sample shown in Figure 3.7.

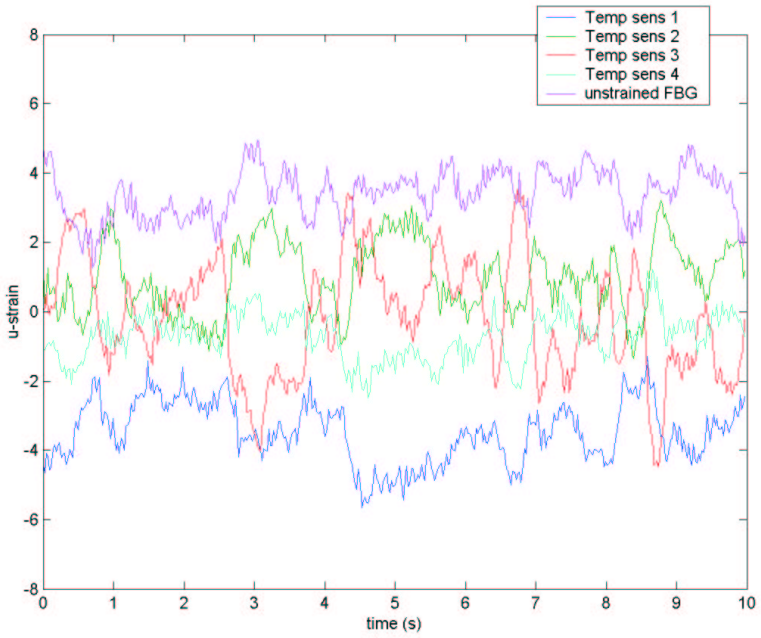

Figure 3.7: The figure shows 5 different gratings measured simultaneously

Sensor	$\epsilon_{max} - \epsilon_{min} (\mu\epsilon)$
Temp sens 1	6.6
Temp sens 2	7.3
Temp sens 3	6.8
Temp sens 4	6.3
Unstrained FBG	4.7

Table 3.3: Polarization dependence of 4 gratings with curvature and one without

First of all, one can notice that all temperature sensors give fairly similar change in strain as a function of SOP. This is expected, since they all have the same curvature and experience the same temperature changes. Even though the unstrained FBG give a smaller change in strain than the temperature gratings, the change is still significant. The cause of the change in strain comes from birefringence introduced by the primary coating (the recoating after the FBG has been written), or from the fiber itself (birefringence introduced under manufacturing).

The DOP from the sources changed significantly from each time it was turned on, which was observed if one looked at the same grating in different measurement series (the source was switched off and on between the series), see Figure 3.8 and Table 3.4

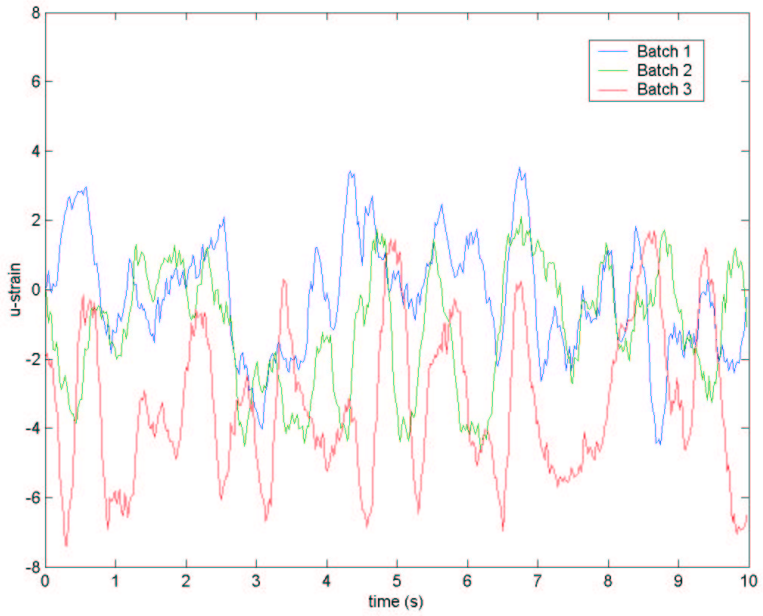

Figure 3.8: The same FBG (temperature stabilized and strain isolated) for 3 different measurement series when the source power has been turned off and on between the measurements

Batch	$\epsilon_{max} - \epsilon_{min} (\mu\epsilon)$
1	8.9
2	6.8
3	9.4

Table 3.4: The polarization dependence in the same FBG, but from different measurement series

Next, we tested different mounting techniques for the grating, see Figure 3.9 and Table 3.5. The first FBG (Blue) is in a flexible but straight lined fiber. The second graph (red/strain FBG 1) shows a grating glued with epoxy (AE10) between two polimide films. The green graph (strain isolated FBG) shows a FBG put in a strain isolated package. This package has

a diameter of 3cm, which consequently introduce a fixed amount of birefringence. The last graph shows a FBG (strain FBG 2) in polimide film glued (Araldite 2010) to a steel plate and covered with glass fiber chopped strand glass matt saturated with vinyl ester.

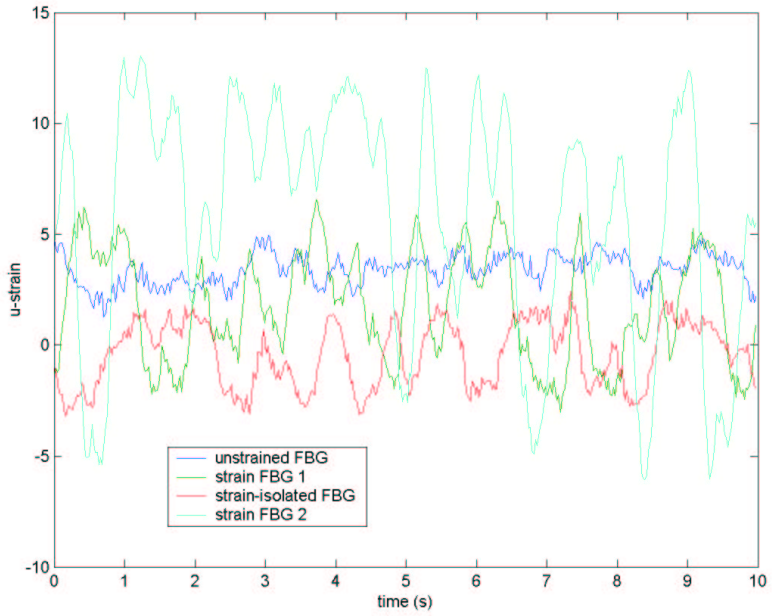

Figure 3.9: The figure shows different FBG mounted in different ways

Sensor	$\epsilon_{max} - \epsilon_{min}\,(\mu\epsilon)$
Unstrained FBG	4.7
Strain-isolated FBG	6.3
Strain FBG 1	10.3
Strain FBG 2	19.9

Table 3.5: Polarization dependence due to different mounting techniqes

Strain FBG 2 was clearly birefringent, and this could also be seen with a spectrum analyzer, since the grating no longer appeared bell shaped.

3.5 Depolarizer

Using depolarized light is one possible solution to minimize the polarization dependence, and is descibed in chapter 2.4. In the following, depolarizers were introduced after the isolator in the hull monitoring system. Strain FBG 2 from the previous section was then tested using no depolarizer, using only one 2x2 coupler (with feedback loop) as depolarizer, and 3 2x2 couplers (with feedback loops) in series as depolarizer, see Figure 3.10 and Table 3.6.

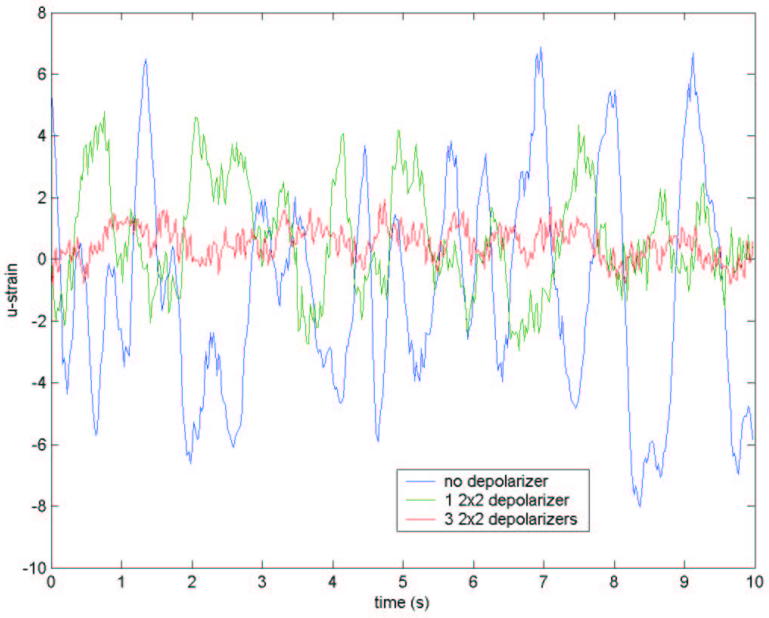

Figure 3.10: Polarization dependence with and without depolarizers

Depolarizer	$\epsilon_{max} - \epsilon_{min}(\mu\epsilon)$
No depolarizer	16.6
1 2x2 depolarizer	8.7
3 2x2 depolarizers	3.5

Table 3.6: Depolarization dependence with different depolarizers

The introduction of the depolarizer shows a significant improvement. One 2x2 coupler reduces the dependence by a factor 2, while 3 couplers in series reduce the dependence almost 5 times. When the light becomes depolarized, the reflected spectrum becomes the average between the two orthogonal axes of polarization instead of “jumping” between the two axis, and this reduce the error introduced by changes in the SOP.

The depolarization effect can also be observed more directly by measuring the DOP with and without depolarizers, see experimental setup in Figure 3.11.

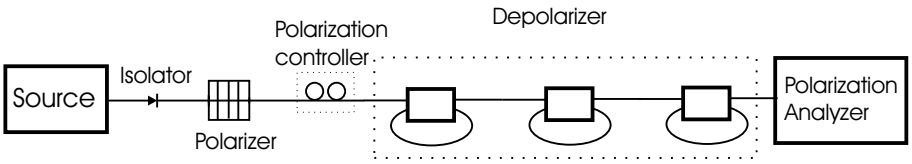

Figure 3.11: Experimental setup of a DOP measurement vs. input polarization

A sample of the measurement is shown in Figure 3.12

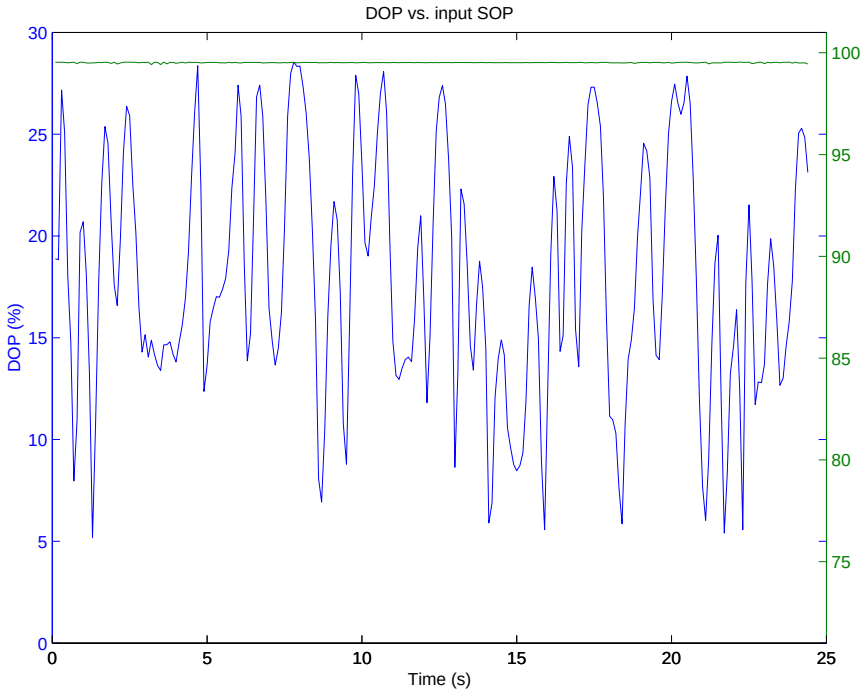

Figure 3.12: Measurement of DOP vs. input SOP with depolarizer (blue graph) and without depolarizer(green graph)

First, one can see that the depolarizers reduced the DOP from $\sim 99\%$ to around 17%. One can also observe that the depolarization factor was dependent of the input SOP, as expected from Chapter 2.4.

4 CONCLUSIONS

It has been shown that the fiber optic hull monitoring system (CHESS II) is polarization dependent when a superluminenscent diode (partially polarized source) is used as light source. Changes in the SOP results in changes in measured strain, and will consequently give a virtual signal. Some birefringence is introduced under manufacturing of fiber and grating (corresponding to $\sim 4\mu\epsilon$ in the CHESS system), and are therefore difficult to avoid. The strain isolated temperature packages and reference gratings (curved gratings) can give an error of $\sim 6 - 7\mu\epsilon$, while the strain gratings can in worst case give error signals above $10\mu\epsilon$. Especially the gratings covered with a glass fiber chopped strand mat show large polarization dependence and consequently give inaccurate results for the strain measurements.

The repeatability of the measurement was poor, and it was difficult to recognize the scan period of the polarization controller. This can indicate that the relation between the output SOP from the polarization controller and the SOP in the grating is not linear as assumed.

A possible solution to the polarization problem has been proposed. Implementing a passive narrow-band depolarizer based on 2x2 couplers is a simple and cost effective way to reduce the polarization dependence. An other solution is using a depolarized source such as the EDFA, but this is a more expensive solution.

References

[1] Wang G, Pran K, Sagvolden G, Havsgård G B, Jensen A E, Johnson G A, Vohra S T (2001): Ship hull structure monitoring using fibre optic sensors, *Smart Materials and Structures* **10**, 472–478.

[2] Sagvolden G, Skaugen A (2002): CHESS II electro–optical unit, technical reference, FFI/RAPPORT-2002/02679, Forsvarets forskningsinstitutt (In Confidence. Distribution limited.

[3] Lee T P, Burrus J C A, Miller B (1973): A stripe-geometry double-heterostructure amplified-spontaneous-emission (superluminescent) diode, *Journal of Quantum Electronics* **QE-9**, 8, 820–828.

[4] Pran K, Sagvolden G, Vines L, Wang G (2002): CHESS fibre optic strain sensor package, FFI/RAPPORT-2002/02642, Forsvarets forskningsinstitutt (In Confidence).

[5] Pran K, Sagvolden G, Torkildsen H E, Vines L (2002): (U) Fibre optic hull monitoring sensor network on KNM Orkla, FFI/RAPPORT-2002/01124, Forsvarets forskningsinstitutt (Restricted. Distribution limited).

[6] Lefevre H (1980): Single-mode fibre fractional wave devices and polarisation controllers, *Electronics Letters* **16**, 778–780.

[7] Bohm K, Petermann K, Weidel E (1983): Performance of lyot depolarizers with birefringent single-mode fibers, *Journal of Lightwave Technology* .

[8] Takada K, Okamoto K, Noda J (1986): New fiber-optic depolarizer, *Journal of Lightwave Technology* **LT-4**, 2, 213–219.

[9] Shen P, Palais J (1999): Passive single-mode fiber depolarizer, *Applied optics* **38**, 9, 1686–1691.

[10] Martinelli M, Palais J (2001): Dula fiber-ring depolarizer, *Journal of Lightwave Technology* **19**, 6, 899–905.

DISTRIBUTION LIST

FFIE **Dato:** 21. August 2002

RAPPORTTYPE (KRYSS AV)	RAPPORT NR.	REFERANSE	RAPPORTENS DATO
X RAPP ☐ NOTAT ☐ RR	2002/3348	FFIE/793/116	21. August 2002
RAPPORTENS BESKYTTELSESGRAD		ANTALL EKS UTSTEDT	ANTALL SIDER
Unclassified		27	25
RAPPORTENS TITTEL		FORFATTER(E)	
POLARIZATION DEPENDENCE IN CHESS FIBER OPTIC STRAIN MONITORING SYSTEM BASED ON FIBER BRAGG GRATINGS		VINES Lasse	
FORDELING GODKJENT AV FORSKNINGSSJEF		FORDELING GODKJENT AV AVDELINGSSJEF:	
Stian Løvold		Johnny Bardal	

EKSTERN FORDELING

ANTALL	EKS NR	TIL
1		Light Structures AS
1		v/Karianne Pran
1		v/Geir Sagvolden
		Postboks 109
		2027 KJELLER
1		FLO/SJØ/T-STA-SK
1		v/OK Arnstein Andreassen
1		v/Atle Sannes
		Postboks 3, Haakonsvern
		5886 BERGEN

INTERN FORDELING

ANTALL	EKS NR	TIL
14		FFI-Bibl
1		Adm direktør/stabssjef
1		FFIE
1		FFISYS
1		FFIBM
1		FFIN
2		Restopplag til biblioteket
		Elektronisk fordeling:
		Gunnar Wang, FFIE
		Øystein Farsund, FFIE
		Lasse Vines, FFIE
		Hans Erling Torkildsen, FFIE
		Atle Skaugen, FFIE

FFI-K1 Retningslinjer for fordeling og forsendelse er gitt i Oraklet, Bind I, Bestemmelser om publikasjoner for Forsvarets forskningsinstitutt, pkt 2 og 5. Benytt ny side om nødvendig.